

# Chapter 15

## X-Ray Core Scanners as an Environmental Forensics Tool: A Case Study of Polluted Harbour Sediment (Augusta Bay, Sicily)

Ian W. Croudace, Elena Romano, Antonella Ausili, Luisa Bergamin and R. Guy Rothwell

**Abstract** Since the 1970s the highly industrialised and enclosed Augusta Bay (Sicily) has become internationally recognized as a polluted environment that could represent a hazard to human health. The pollutant of greatest concern, derived from a former chlor-alkali plant, is mercury that exists beyond Intervention Levels in parts of the harbour. The affected areas are also contaminated by other heavy metals and organic compounds (PAHs and PCBs) that were mainly discharged from co-located petrochemical industries. Several previous investigations established the magnitude of particular contaminants in sediments and evaluated the impact of the pollution on a range of biota. The current study, which represented part of a larger project managed by the Italian Environmental Research Institute ISPRA, was concerned with investigating a series of cores collected across the harbour area to establish reliable pollution chronologies based on elemental and radiochronological ( $^{137}\text{Cs}$ ) profiles. The declared motivation for the main project was to acquire scientific evidence that could be used to support a legal investigation against the industries that caused the pollution and who could potentially be expected to contribute to remediation costs. Undisturbed cores were collected from the northern (mildly polluted), central (significantly polluted) and southern (strongly polluted) parts of the Bay using available bathymetric data to avoid areas affected by dredging. The study has demonstrated the value of using an automatic, X-ray sediment core scanner (Itrax) to acquire high-resolution geochemical data. The Itrax provided a non-destructive, sensitive and rapid capability to systematically analyse a broad range of major and trace elements. One of the collected cores of this study, taken from the most polluted site,

---

I. W. Croudace (✉)

Ocean and Earth Science, National Oceanography Centre, University of Southampton,  
Waterfront Campus, European Way, Southampton SO14 3ZH, UK  
e-mail: iwc@noc.soton.ac.uk

E. Romano · A. Ausili · L. Bergamin

Istituto Superiore per la Protezione e Ricerca Ambientale (ISPRA),  
Via Vitaliano Brancati, 60, 00144 Roma, Italy

R. G. Rothwell

National Oceanography Centre, Empress Dock, Southampton, SO14 3ZH, UK

© Springer Science+Business Media Dordrecht 2015

I. W. Croudace, R. G. Rothwell (eds.), *Micro-XRF Studies of Sediment Cores*,

Developments in Paleoenvironmental Research 17, DOI 10.1007/978-94-017-9849-5\_15

provided more than 20 continuous elemental profiles with depth (e.g. Ti, S, Ca, K, Mn, Fe, Cr, V, Ba, Cu, Zn, Br, Rb, Sr, Zr, Hg, Se, Mo). The Itrax data quality were validated against a dataset acquired using a conventional WD-XRF instrument and both sets of profiles are demonstrated to be consistent. This ability of the Itrax to automatically scan cores over a significantly shorter time compared to conventional laboratory methods (days compared to weeks) confirms its potential in contributing to environmental forensic studies. Its additional ability to simultaneously record a radiographic image (and radiographic digital profile) provides a link between sediment layering (density variations linked to mineralogy) and elemental composition.

**Keywords** Environmental forensics · Mercury pollution · Heavy metal pollution · Augusta Harbour · Mercury-cell chloralkali plant · Itrax core scanning

## Introduction

Significant environmental pollution arising from past industrial practices is a worldwide concern. In the European context, with relatively well-developed environmental guidelines and regulatory systems, the legacy of industrial contamination continues to be progressively targeted for evaluation and eventual remediation. The EU's Environmental Liability Directive 2004/35/EC applies the 'polluter pays' principle to prevent and remediate environmentally damaged land, water and natural habitats to ultimately ensure biosphere protection. Therefore, during early investigations of legacy contaminated sites specialist evidence needs to be established to contribute robust evidence to identify potential polluters. As investigations progress, regulatory agencies often employ internal scientific and other expertise but they may also employ independent external specialists. Where there is legal oversight and a potential criminal link the overall study approach has been termed *Environmental Forensics*. This recently emergent field has its own specialist society and a professional journal and it draws together relevant branches of chemistry (analytical, aquatic, atmospheric, geochemistry) and environmental science (ecology, transport and fate of contaminants) to address legal aspects of environmental contamination. The term has become more widely used to describe investigations where complex scientific evidence is used to apportion responsibility for instances of pollution to the satisfaction of a court (see for example Hester and Harrison 2008). A notable early reference to *Environmental Forensics* was associated with the legal investigation of the disastrous Exxon Valdez oil spill in 1989.

Given the complexities of how pollutants behave and impact on the environment multidisciplinary investigative approaches are invariably required. Establishing pollution histories in aqueous environments for example, normally involves the collection and investigation of sediment cores (e.g. Croudace and Cundy 1995;

Cearreta et al. 2002; Cundy et al. 2003). In this context, the introduction of high-resolution core scanners has provided a technical advance that allows rapid and non-destructive analysis. These new analytical tools, of which two proprietary instruments dominate the market (Croudace and Rothwell 2015), have stimulated research output in the environmental sciences (e.g. Croudace et al. 2006; Lepland et al. 2010; Croudace et al. 2012; Miller et al. 2014, 2015). A particular strength of the Itrax core scanner is its co-registration of radiographic and elemental profiles as well as an optical image.

**Augusta Bay** The highly industrialised Augusta Bay in eastern Sicily has been the focus of environmental investigations for over four decades as it became clear that the area was seriously polluted from multiple sources. Numerous studies have reported on the impact and scale of pollution in the area (e.g. Sciacca and Fallico 1978; Castagna et al. 1985; Ausili et al. 2008, 2012; Bellucci et al. 2012; Romano et al. 2009b, 2013; WHO 2012; **Text Box 15.1, 15.2 and 15.3**). This current Augusta Bay study arose from a project commissioned and managed by the Italian Institute for Environmental Protection and Research (ISPRA). The project was associated with a broader legal investigation by the Siracusa Prosecutor's Office into identifying, where possible, the companies that might have caused pollution in Augusta Harbour. The approach used was to acquire geochemical and chronological data from a set of sediment cores with the intention of establishing a pollution chronology. The cores were collected by ISPRA, in duplicate, from different parts of the Harbour with the purpose of investigating heavy metals, organic pollutants and selected radionuclides.

### **Text Box 15.1 Industrial pollution history of Augusta Harbour**

Augusta Harbour sediments are significantly affected by past and present industrial activities having high concentrations, varying with depth, of mercury, barium sulphate, hydrocarbons, hexachlorobenzene (HCB), PCBs, dioxins and furans.

**1950** First construction of oil refineries.

**1958** Chlor-alkali plant begins operation.

**1960s** Closure of the Bay by an artificial wall to protect shipping and large industrial expansion

**1958-2003** The chlor-alkali plant and other industries are significantly operational and ~500 t of Hg was estimated to have been discharged to the Harbour.

**1980** Installation of a de-mercurisation plant.

**2005** Chlor-alkali plant closed and Hg cells removed.

**2011** Proposal to remediate Augusta Harbour (e.g. Guerriero et al. 2011).

**Text Box 15.2 The mercury cell chlor-alkali process**

The mercury cell industrial process has been in use for well over 100 years and involves the electrolysis of a NaCl brine to produce chlorine and sodium hydroxide both critical precursors in different aspects of industrial chemistry. In the process, also known as the Castner-Kellner process, a saturated brine solution floats on top of a thin layer of Hg (cathode). During electrolysis, chlorine was produced at the anode and sodium at the cathode forming a sodium-mercury amalgam that was continuously drawn out of the cell and reacted with water to produce sodium hydroxide. The Hg was recycled back into the electrolytic cell. It was very important to remove chemical impurities (Ca, Mg, sulphate, etc.) from the brine before electrolysis otherwise they adversely affected the efficiency of the process. Removing sulphate was typically achieved using barium chloride and the barium sulphate produced could also have become a waste product. If brine purification was inadequate then so-called ‘mercury butter’ formed that led to short circuits, poor mercury flow, increased power consumption and increased exposure to mercury vapour (Sedivy 2009). Over time, sludges formed that required extraction and disposal and at many poorly managed plants these may have been simply discharged to the environment.

Around 2005 it was estimated that European mercury cell chlor-alkali plants (MCCAPs) consumed 175–200 t/year of mercury, amounting to 40–50% of the total EU mercury consumption. By contrast, modern chlor-alkali plants, that use ion-selective membranes (considered to be ‘best-available-technology’) use no mercury and are far more energy efficient.

**Global mercury elimination:** In 2009, UNEP Global Mercury Partnership Advisory Group reported that 44 countries still had 100 facilities with some industrial mercury cell chlorine capacity. The European chlor-alkali industry, represented by EuroChlor, declared they would phase out all mercury-cell chlor-alkali units by 2020 while the USA planned to close its four remaining mercury cell facilities by the end of 2018. In India, mercury-cell chlorine production was intended to cease by 2012 (Anirudh et al. 2009). Through international agreement coordinated by UNEP it is imminently expected that all 193 nations in the UN will have signed the *Minimata Convention on Mercury* which aims to reduce and ultimately eliminate mercury emissions in the environment (<http://www.unep.org/hazardoussubstances/MinamataConvention>; accessed Oct 2013).

**Text Box 15.3 Selected reports from a chemical industry news service****EniChem Priolo (Sicily) chloralkali plant shuts following pollution arrests—17 January 2003—Source: ICIS news LONDON (CNI)****(International Chemical Information Service—Chemical News and Intelligence)**

The Italian police confirmed Friday that they have arrested 18 people, including 17 EniChem executives, on charges of environmental pollution and criminal conspiracy in connection with the company's Priolo, southern Italy chemicals complex. The executives and a local government official are accused of breaking the Ronchi decree DL 22/1997 on industrial pollution, according to Ten. Col. Giovanni Monterosso, the head of the Siracusa, Sicily district financial police. Local reports suggest the charges relate to improper disposal of untreated, toxic mercury waste into the sewer system at Priolo, where EniChem and its subsidiary Polimeri Europa have extensive petrochemical installations, including caustic soda, chlorine and aromatics plants. Among those arrested are the former plant director and deputy plant director, who were responsible for the plant at the time of the alleged incident about a year ago; the current Priolo plant director and local government official in charge of pollution control. Other EniChem executives arrested are responsible for environment and safety, records, special waste disposal, chemical laboratory, chlor-alkali production and aromatics. They have all chosen to be represented by EniChem lawyers. Eight of the executives were held in jail and ten were placed under 'home arrest' following dawn raids on Thursday. In a statement, EniChem said it hopes the investigation throws light on the matter. It added: "EniChem and Polimeri Europa would like to point out that until this day the operative structure was run in respect of the law".

**21 January 2003—Source: ICIS news LONDON (CNI)**

Chloralkali production at EniChem's Priolo site in Sicily has been halted temporarily following the arrest of senior managers on pollution charges, a company spokeswoman confirmed to *CNI* on Tuesday. EniChem said that "the decision to halt production at the site was taken in order to guarantee safety at the plant and follows the absence of key personnel". The spokeswoman said the plant was closed last Friday (17 January), a day after 17 senior managers were arrested on charges of environmental pollution and criminal conspiracy. The 700 workers employed at the plant are now engaged in activities of "extraordinary maintenance", the spokeswoman added. She said she could not forecast a date for the resumption of operations at the site but said that no other units had been affected by the temporary closure.

**Industrialisation** Augusta Bay (Figs. 15.1 and 15.2) developed into a significant industrial Mediterranean harbour from the 1950s onward and became a major processing centre for petrochemicals and chemical industry precursors. The high concentration of these industries and their discharges imposed a pollution legacy on the Bay

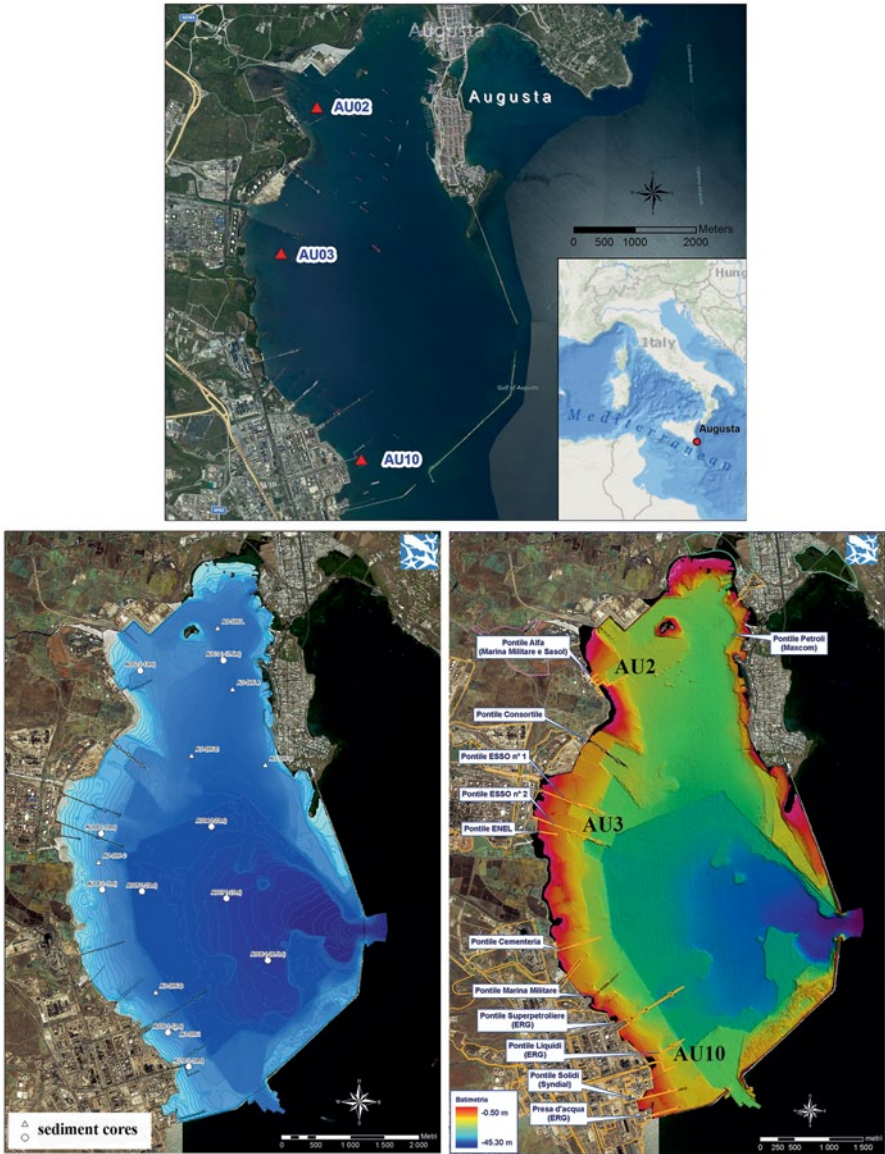


Fig. 15.1 Location of sampling areas for AU2, AU3 and AU10 different cores, in the industrialised Augusta Harbour along with *bottom contours* indicating dredged areas

that has become a significant concern. Pressures to industrially develop the area after the Second World War and the lack of an appropriate environmental law led to many cases of poor ecological control. Further industrial development followed the construction of the breakwaters that closed the bay and also the dredging of the harbour in the early 1960s. The harbour area is 8 km long and 4 km wide with a mean water

**Fig. 15.2** Industrial views of parts of Augusta Harbour, Sicily. (*photos courtesy of E. Romano*)



depth of 14.9 m and is characterized by poor water circulation. Several industries such as chemical and petrochemical plants, oil refineries and electric power plants have impacted the area for several decades, but one of the most important contributors of hazardous waste to the Harbour was from a mercury cell chlor-alkali plant (MCCAP) that operated from 1958 to 2003.

It is estimated that over 500 t of untreated Hg waste entered the harbour from 1958 to 1979 along with by-products from the brine purification process linked to the MCCAP. Mercury mitigation measures were introduced at Augusta in the late 1970s and by 2005 the mercury cells were finally removed. From the 1970s it was clear that significant environmental degradation had occurred (Sciacca and Fallico 1978; Cernigliaro et al. 2008; Bellucci et al. 2012). Uncontrolled pollution had led to significant contamination of sediment by heavy metals, polychlorobiphenyls (PCBs), polycyclic aromatic hydrocarbons (PAHs) and hexachlorobenzene (HCB) most significantly in the southwestern part of the Harbour. Since the closure of the chloralkali plants there has been some recovery but sub-surface sediments remain adversely contaminated and mercury (Hg) contamination continues to be an environmental concern. Subsequent and regular monitoring programs were used to determine potential transfers of the Hg to the ecosystem and to establish the extent of contamination as a precursor to possible remediation (Guerriero et al. 2011).

Recent studies of the area have established the vertical and spatial distributions of some heavy metals (Hg and Ba), PAHs, HCB and PCBs in the Harbour and found the highest concentrations in the southern sector. Particularly, Hg was found up to 190 mg kg<sup>-1</sup> dwt in superficial sediments, and exceeding 500 mg kg<sup>-1</sup> dwt in the upper 50 cm sediment interval (ICRAM 2008; Romano et al. 2009b, 2013). Off-shore sediments collected close to the Harbour showed considerable anthropogenic enrichment of Hg (EF > 40) and adverse response of benthic communities in terms of faunal density and incidence of morphological deformations (Di Leonardo et al. 2006, 2014). One study argued that the high Hg content in the Harbour sediments were important contributors for this element to the Mediterranean Sea, with an Hg output of 0.162 kmol/year to coastal and offshore waters (Sprovieri et al. 2011). Clear health concerns developed when it became clear that high Hg was accumulating in local sediment based on known serious impacts elsewhere (e.g. Minamata, Japan; Tomiyasu et al. 2006; Clarkson 1997). Bioavailable methyl mercury was expected to be present in the sediments as had been recorded around other Italian and European chlor-alkali plants (Covelli et al. 2001, 2009, 2010; Piani et al. 2005; Raldúa et al. 2007). Studies involving mercury in marine organisms from Augusta Harbour indicated a clear toxicological risk. Pregnant women were identified as an exposed group (Ausili et al. 2008) based on the incidence of neonatal malformations which were found to be more than three times higher than the Italian national average (Bianchi et al. 2004).

**Sediment Character** The character of sediment found in the Harbour reflects the local geology, soil composition and the hydrological catchment. The local geology consists of carbonate sequences (Cretaceous to Quaternary Age), with volcanoclas-

tic and volcanic interbedded horizons along with muddy sediments and calcarenites (Nigro and Renda 2000; Scicchitano et al. 2007). Three small streams flow into the western part of the harbour, but their freshwater and sediment flows are generally considered to be rather small (Celia Magno et al. 2012). In the southernmost part of the harbour patchy areas of emerging rocky substrate are present near the shore (Anonymous 1992, 1995). Weathering and fluvial transport of this mixed material into the harbour during periods of significant rainfall provides the main source of Harbour sediment.

## Methods

### *Sampling*

Seven sediment cores were collected from three stations (AU2, AU3 and AU10) in July 2008 located in the northern, central and southern part of the Harbour respectively (Fig. 15.1, Table 15.1). Two replicates were collected at stations AU2 and AU3, while three replicates were taken at AU10 station. Stations were carefully selected from areas identified from bathymetric survey data to be most likely to be unaffected by dredging. Two types of sediment corers were used, (a) an SW-104 gravity-corer (patented by the Italian Council of Research) specifically designed to minimize disturbance and preserve an optimal sediment/water interface and (b) a Rossfelder® vibrocorer. The latter was used to obtain longer cores when the gravity corer was unable to achieve significant penetration when encountering pebbly horizons/bedrock. Comparison of vertical chemical profiles obtained using the two corers offered a check on any possible disturbance of the sedimentary sequence

**Table 15.1** Summary of collected cores and analyses carried out for this study

Core label	Coordinates	ISPRA analyses	GAU analyses
AU2g <sub>iwc</sub>	4120496 N–517400 E		Dating, WD-XRF
AU2g <sub>er</sub>	4120498 N–514702 E	Grain size, Hg, PAHs, PCBs	Dating, WD-XRF
AU3g <sub>iwc</sub>	4118104 N–516811 E		Dating, WD-XRF
AU3v <sub>er</sub>	4118106 N–516813 E	Grain size, Hg, PAHs, PCBs	Dating, WD-XRF
AU10g <sub>iwc</sub>	4114716 N–518128 E		Dating, WD-XRF
AU10v <sub>iwc</sub>	4114715 N–518126 E		Dating, WD-XRF, Itrax
AU10v <sub>er</sub>	4114714 N–518126 E	Grain size, Hg, PAHs, PCBs	Dating, WD-XRF

v—vibro corer sample, g—gravity corer sample

caused by sampling. All cores were immediately sub-sampled by ISPRA after collection with the exception of AU10<sub>v<sub>iwc</sub></sub> which was sent directly to the Southampton GAU laboratories for Itrax analysis and radiochronological determinations. Gravity cores were sub-sampled by extrusion, while the vibrocores were sampled following longitudinal splitting. Samples for geochemical, grain size and radiochronological dating were carried out on 1-cm and 3-cm resolution samples. Sediments were stored/preserved in polyethylene bags in a freezer before analysis.

### ***Grain Size, Trace Elements and Organic Compounds Analyses***

***Grain-size analysis*** was carried out treating sediment sample with a 30% H<sub>2</sub>O<sub>2</sub> solution and separating it into coarse (>63 μm) and fine (<63 μm) fraction by wet sieving. Then, each fraction was dried and the coarse one was fractionated using ASTM series sieves, while the fine fraction was analyzed using a laser granulometer that determines silt and clay fractions separately (Romano et al. 2009a).

***Barium*** was analyzed using wavelength dispersive X-ray fluorescence analysis (WDXRF) by the Southampton Group (GAU).

***Mercury*** was analyzed at ISPRA on wet samples by means of a Direct Mercury Analyzer (DMA-80, FKV) through thermal desorption, gold amalgamation and atomic absorption without any chemical pre-treatment (EPA method 7473). Quantification limit was 0.0005 mg kg<sup>-1</sup> on a dry weight basis. Itrax and WD-XRF were also used to measure Hg and the data were found to correlate with the DMA-80 data (Maggi et al. 2009).

***Polycyclic Aromatic Hydrocarbons (PAHs)*** analyses were performed by a preliminary extraction and a successive purification on silica gel treatment. Successively, the determination was carried out using an Agilent 1100 HPLC-FLD system managed through the Chemstation software (Romano et al. 2009a). The quantification limit was 0.001 mg kg<sup>-1</sup>.

***Polychlorobiphenyls (PCBs)*** were analysed as <2 mm homogenised, freeze dried samples and then extracted by pressurized fluid extraction using a Dionex model ASE 200 instrument. The determination was performed by high-resolution gas chromatography with electron capture detection (GC/ECD) in dual column-dual detector mode. The limit of quantification was 0.0001 mg kg<sup>-1</sup> on a dry weight basis. On each extraction batch a method blank, a spiked blank for recovery evaluation and sample replicates and CRMs were analysed to ensure quality control (Bergamin et al. 2009).

***Itrax non-destructive core scanning*** was carried out on a split core of AU10<sub>v<sub>iwc</sub></sub> in Southampton. The key components of this instrument comprise a 3 kW Mo-target sharp, fine-focus X-ray tube coupled to a 0.2 × 20 mm rectangular capillary wave guide, a silicon-drift detector and an X-radiographic linear diode detector (Croudace et al. 2006). Along core profiles are presented as variation in counts (Fig. 15.3) that provide a reliable proxy for element concentration variations (see

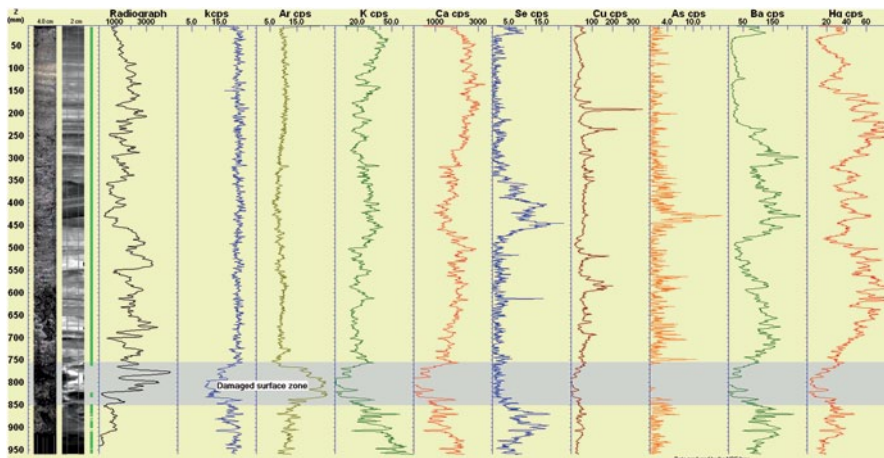


**Fig. 15.3** AU10<sub>v\_1wc</sub> (0–950 mm) elemental and radiographic data obtained using the Itrax core scanner. The figure was generated using ItraxPlot software (see Chap. 26). The small gap in the data at 750–850 mm is due to unreliable data caused by a poor sediment surface where hydrocarbon-rich, soft muddy sediment was slightly depressed. Poor surfaces result in erroneous detector counts

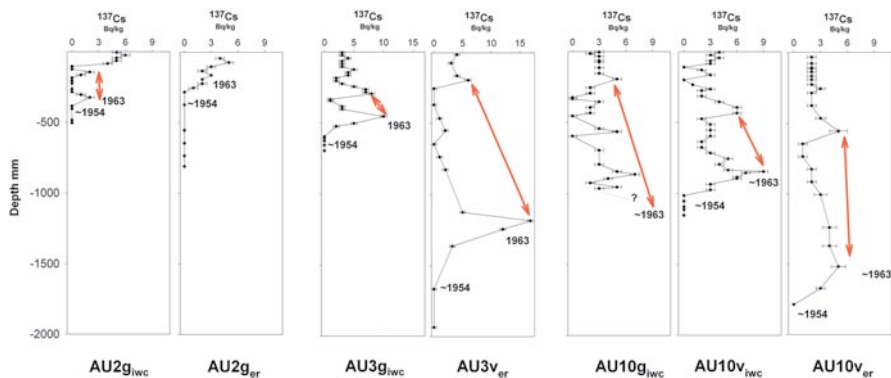


**Fig. 15.4** Cs-137 (Bq/kg) profiles for cores from locations AU2, AU3 and AU10. The red double-ended arrowed line marks out two recognizable features seen in most of the cores regardless of their accumulation rate (1963 ‘bomb’ maximum and possible 1986 Chernobyl event). The recovery of core AU10<sub>g</sub> was too short to see the 1963 ‘bomb’ maximum

Figs. 15.7 and 15.8). The Itrax collected X-ray fluorescence spectra at 200 μm intervals (approximately 5000 X-ray spectra are recorded per metre of core) leading to 20 element profiles (As, Ba, Br, Ca, Cl, Cr, Cu, Fe, Hg, K, Mn, Mo, Pb, Rb, S, Se, Sr, Ti, V, Zn).

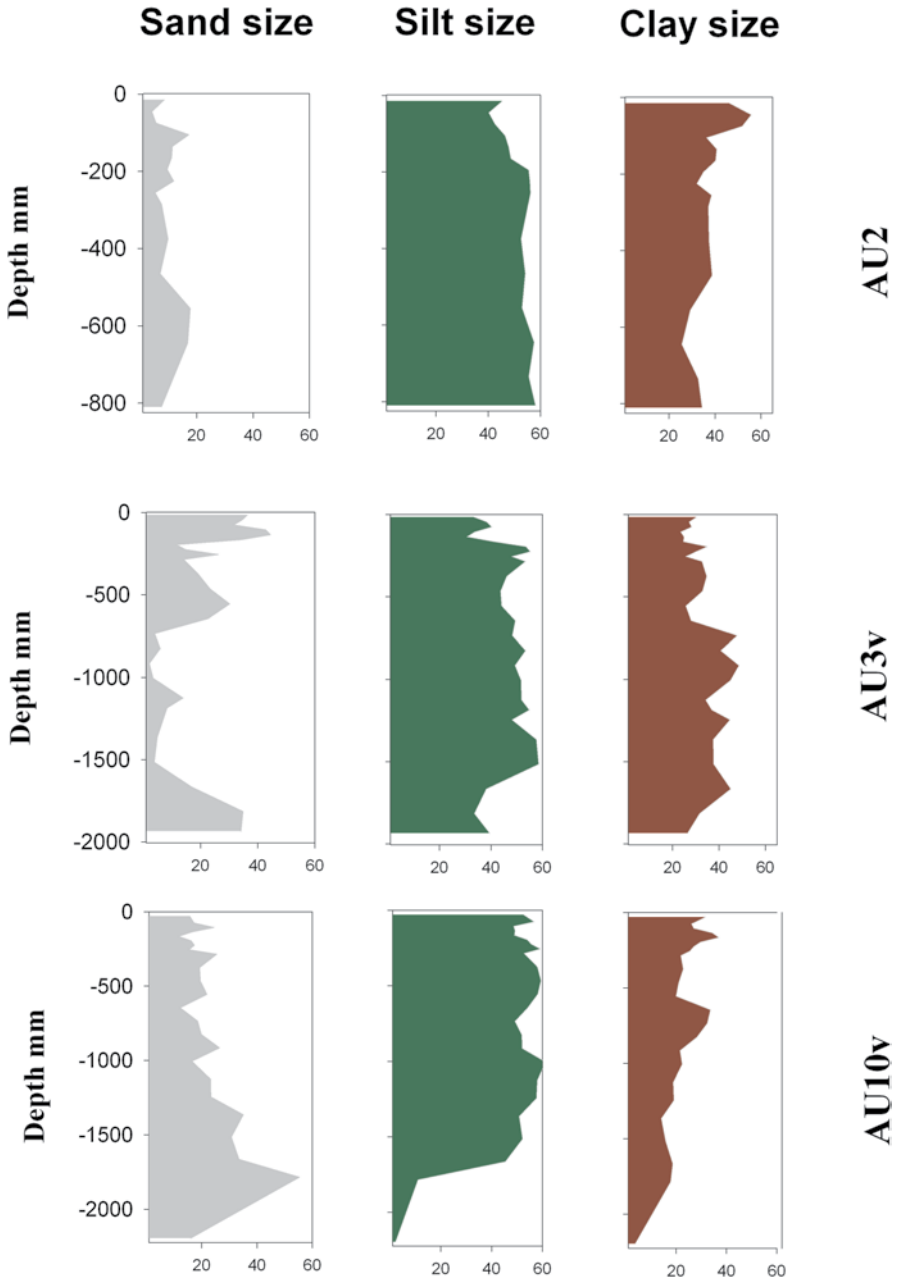


Fig. 15.5 Grain-size variations with depth for cores from locations AU2, AU3 and AU10v

*WD-XRF Elemental Analysis* General elemental geochemistry (major elements and trace elements) on sediment core material was carried out using a Panalytical Magix-PRO WD-XRF spectrometer in Southampton. The instrument employed a 4 kW Rh end-window X-ray tube and the system quantitatively analysed sub-samples taken at 1-cm increments. All samples were ground and pelletised prior to analysis. The WD-XRF system had been previously calibrated using a suite of more than 20 international geochemical reference samples provided by CRPG-ANRT, USGS, JGS and CANMET. Accuracy was assessed by running the reference samples MESS-3, PACS-2 and MAG-1 and measured data were generally within 5–10% of the consensus values. Detection limits for low-medium Z elements are 5–20 mg kg<sup>-1</sup> and for medium-high Z elements they are approximately 1–5 mg kg<sup>-1</sup>.

*Radiochronological Determinations* Caesium-137 was measured using well-type ULB HPGe gamma spectrometry systems (Canberra Instruments, UK) in Southampton. All systems were calibrated using NPL certified mixed gamma solution. Samples were counted in scintillation vials for 100,000 s and analysed using Fitz-peaks gamma analysis software (JF Computing, Stanford in the Vale, UK).

## Results

A general impression of the variations in sediment geochemistry, derived from WD-XRF analysis, including anthropogenic elements (Ag, As, Ba, Ca, Co, Cr, Cu, I, Mo, S, Se, Sr, Zn) is provided in Table 15.2. For comparison, data for a typical uncontaminated marine muddy sediment (the well characterized USGS MAG-1 reference sample) allows the extent of pollution in the various cores to be evaluated. It is recognised that MAG-1 is a carbonate poor sediment but such a mineralogical composition is considered similar to one of the components of the Augusta sediment (Fig. 15.6). Mineralogically, uncontaminated Augusta sediment consists largely of two components, a calcium carbonate (Ca and Sr) and clays (Si, Al, K, Rb). Polluted sediment includes additional components (typically less than 6 wt%) such as barite, hydrocarbons and sulphides. Where there are significant down-core geochemical variations in major mineral components then elemental profiles will be influenced by the closed-sum effect (Rollinson 1993). With this effect, caused by analyses summing to 100%, any variation in one major mineral component (e.g. Ca and Sr in carbonates) will affect the other mineral components (e.g. Si, K, Al, Rb, Si in clay). The use of element ratios (e.g. dividing elements associated with clays by Al<sub>2</sub>O<sub>3</sub>, K<sub>2</sub>O, Rb etc) can compensate for the closed-sum effect and negate the effect of calcium carbonate variations. In this case K<sub>2</sub>O was used as the normalising element (Figs. 15.6 and 15.11).

Radiochronological dating inferred from <sup>137</sup>Cs measurements was performed on sub-samples from all cores (Fig. 15.8). Grain-size data from sub-samples taken from the cored sediment show variations (Fig. 15.5) that are reflected in the geochemistry to some extent.

**Table 15.2** Geochemical data for Augusta sites AU2 (mildly polluted), AU3 (significantly polluted) and AU10 (strongly polluted). (data from Govindaraju 1994)

	AU2						AU3						AU10						USGS MAG-1
	Mean	SD	Min	Max	Median		Mean	SD	Min	Max	Median		Mean	SD	Min	Max	Median		
SiO <sub>2</sub>	38.03	1.01	35.95	39.60	38.22		31.75	2.95	28.21	36.56	30.64		10.24	8.65	0.09	56.12	9.52	50.36	
TiO <sub>2</sub>	1.59	0.06	1.44	1.69	1.59		1.56	0.11	1.32	1.73	1.58		0.49	0.10	0.26	0.78	0.51	0.75	
Al <sub>2</sub> O <sub>3</sub>	12.08	0.44	11.06	12.72	12.15		11.03	1.03	9.70	13.08	10.62		5.91	2.19	2.73	16.24	5.81	16.37	
Fe <sub>2</sub> O <sub>3</sub>	8.21	0.33	7.62	8.79	8.23		7.50	0.69	6.64	8.61	7.27		5.46	1.17	3.55	8.31	5.29	6.80	
MnO	0.07	0.00	0.06	0.07	0.07		0.07	0.01	0.06	0.09	0.07		0.04	0.01	0.03	0.11	0.04	0.10	
MgO	3.13	0.13	2.90	3.29	3.16		2.94	0.12	2.69	3.24	2.94		3.08	0.53	1.94	4.35	3.17	3.00	
CaO	17.64	1.31	15.88	20.40	17.28		25.19	4.13	18.52	30.53	26.52		44.28	8.99	1.53	56.24	44.96	1.37	
K <sub>2</sub> O	1.45	0.07	1.29	1.56	1.46		1.14	0.18	0.86	1.43	1.11		0.89	0.52	0.40	3.78	0.82	3.55	
Na <sub>2</sub> O	3.40	0.68	2.77	5.51	3.14		3.30	0.28	2.84	3.92	3.23		2.00	0.45	1.23	3.11	1.89	3.83	
P <sub>2</sub> O <sub>5</sub>	0.25	0.01	0.23	0.28	0.25		0.27	0.02	0.24	0.32	0.27		0.56	0.22	0.11	0.91	0.62	0.16	
Cl	2.87	0.91	2.12	5.99	2.57		2.62	0.17	2.29	3.04	2.64		2.73	0.88	0.94	4.27	2.81	3.10	
Ag	mg kg <sup>-1</sup>	<2	<2	<2	<2		<2	<2	<2	<2	<2		10	4	5	17	8	0.08	
As	mg kg <sup>-1</sup>	19	2	17	26	19	14	2	11	20	14		20	4	11	31	19	9.2	
Ba	mg kg <sup>-1</sup>	254	40	176	321	256	275	59	182	434	280		1.53%	1.15%	0.05%	4.22%	0.99%	479	
Br	mg kg <sup>-1</sup>	115	39	69	229	112	99	20	64	140	101		223	80	52	331	242	252	
Co	mg kg <sup>-1</sup>	32	1	31	34	32	30	3	26	35	30		72	31	24	137	75	20	
Cr	mg kg <sup>-1</sup>	133	7	121	147	133	164	37	129	269	151		192	88	88	428	148	97	
Cu	mg kg <sup>-1</sup>	55	17	33	85	53	52	18	33	103	45		415	211	27	838	428	30	
Ga	mg kg <sup>-1</sup>	16	1	12	17	16	14	1	12	16	14		10	3	6	23	10	20	
Hg	mg kg <sup>-1</sup>	0.9	0.6	0.1	1.8	0.9	3	3.4	0.1	16.7	2.0		518	138	311	728	415	0.018	
I	mg kg <sup>-1</sup>	85	23	52	140	85	76	33	49	164	62		79	61	22	409	72	380	
Mo	mg kg <sup>-1</sup>	<2	<2	<2	<2	<2	6	3	2	12	4		65	59	0	210	50	1.6	
Ni	mg kg <sup>-1</sup>	48	3	43	53	49	51	10	37	67	51		19	7	7	35	19	53	

Table 15.2 (continued)

	AU2						AU3						AU10						USGS MAG-1		
	Mean	SD	Min	Max	Median	Mean	SD	Min	Max	Median	Mean	SD	Min	Max	Median	Mean	SD	Min		Max	Median
Pb	mg kg <sup>-1</sup>	24	8	10	35	25	42	47	208	23	50	16	14	75	56	50	16	14	75	56	24
Rb	mg kg <sup>-1</sup>	46	4	39	51	46	34	8	49	32	29	22	14	153	26	29	22	14	153	26	149
S	mg kg <sup>-1</sup>	18,013	4224	9937	22,470	19,297	16,815	2674	23,826	16,775	29,981	11,186	5136	49,585	31,755	29,981	11,186	5136	49,585	31,755	3900
Se	mg kg <sup>-1</sup>	<2	<2	<2	<2	<2	<2	<2	<2	<2	14	14	1	55	8	14	14	1	55	8	1.16
Sr	mg kg <sup>-1</sup>	481	56	381	562	490	581	129	905	582	1190	281	143	1616	1248	1190	281	143	1616	1248	146
V	mg kg <sup>-1</sup>	151	10	128	169	149	154	14	199	151	137	25	89	192	142	137	25	89	192	142	140
Y	mg kg <sup>-1</sup>	31	1	30	33	32	31	1	33	31	51	16	19	81	55	51	16	19	81	55	28
Zn	mg kg <sup>-1</sup>	107	26	73	149	102	99	31	149	90	223	80	61	386	242	223	80	61	386	242	130
Zr	mg kg <sup>-1</sup>	196	7	177	206	197	173	19	203	175	51	21	17	137	51	51	21	17	137	51	130
PCB	mg kg <sup>-1</sup>	0.016	0.010	0.001	0.032	0.019	0.058	0.068	0.197	0.016	6.520	3.157	0.299	14.005	6.169	6.520	3.157	0.299	14.005	6.169	n/a
PAH	mg kg <sup>-1</sup>	0.38	0.09	0.16	0.49	0.38	0.89	1.07	4.19	0.37	25.61	11.96	6.90	47.70	25.90	25.61	11.96	6.90	47.70	25.90	n/a

USGS reference sample MAG-1 is used as an exemplar of a typical unpolluted (though non-calcareous) muddy sediment

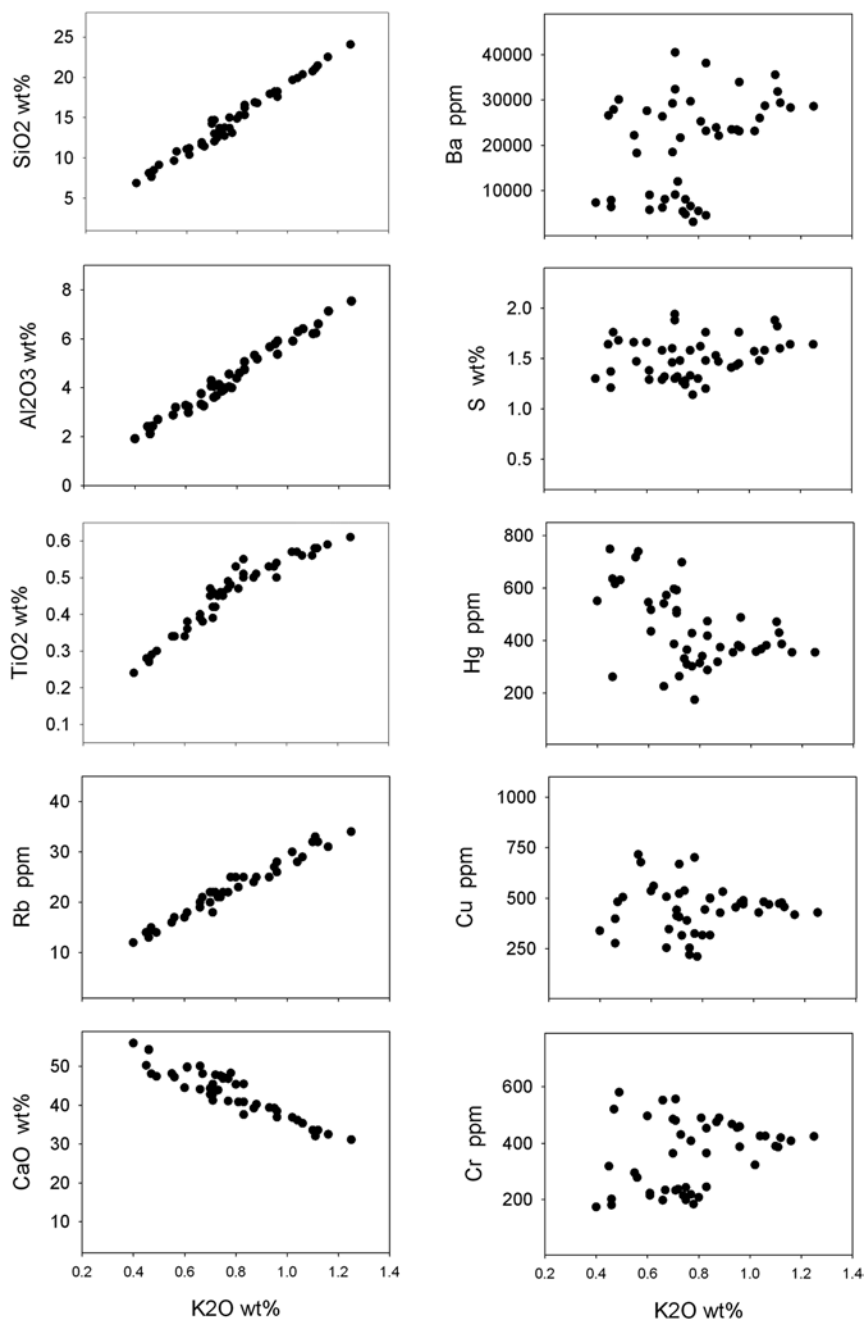


**Fig. 15.6** Elemental bi-plots for AU10v<sub>iwc</sub>. The main components of dried sediment are clay and calcium carbonate minerals. Other components (<5 wt% dry sediment) include sea salts and anthropogenic barium sulphate, calcium sulphate and hydrocarbons

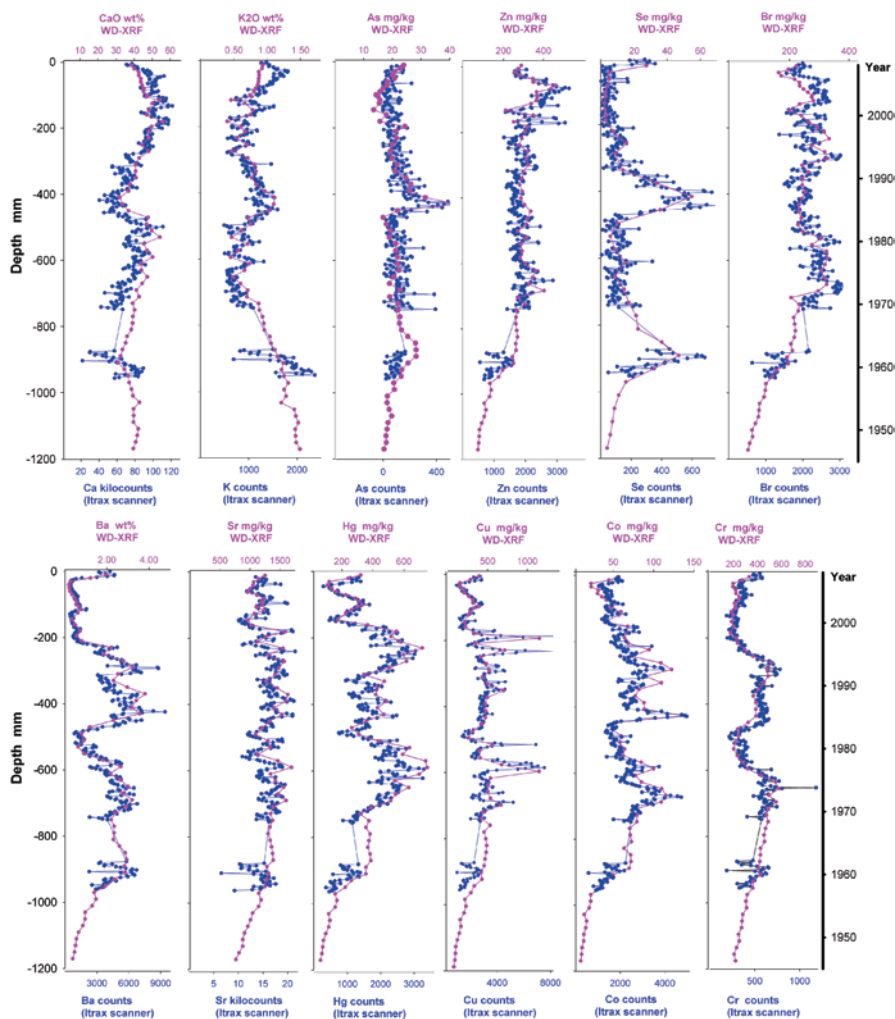


**Fig. 15.7** Comparison of Itrax (blue line, 200  $\mu\text{m}$  scanning resolution) and WD-XRF data (red line, 1-cm sampling resolution) for AU10<sub>v</sub><sub>1w</sub>. The Itrax data are plotted as 5-point means. The right axis represents the Year based on the 137Cs chronology

**Site AU2** No significant variations in grain-size were recorded with depth and the sediment is mainly composed of silt with the highest content (58%) at the core bottom (Fig. 15.5). The upper interval from 0 to 7.5 cm depth has clay > silt. Sand-sized material ranges from 4 to 18% while gravel is absent. The two cores collected for sediment geochemistry analyses (AU2<sub>g<sub>cr</sub></sub> and AU2<sub>g<sub>1w</sub></sub>) are generally similar and have a comparable accumulation rate. The uppermost 50 cm of sediment show only limited contamination of PCBs and Hg (Fig. 15.8).

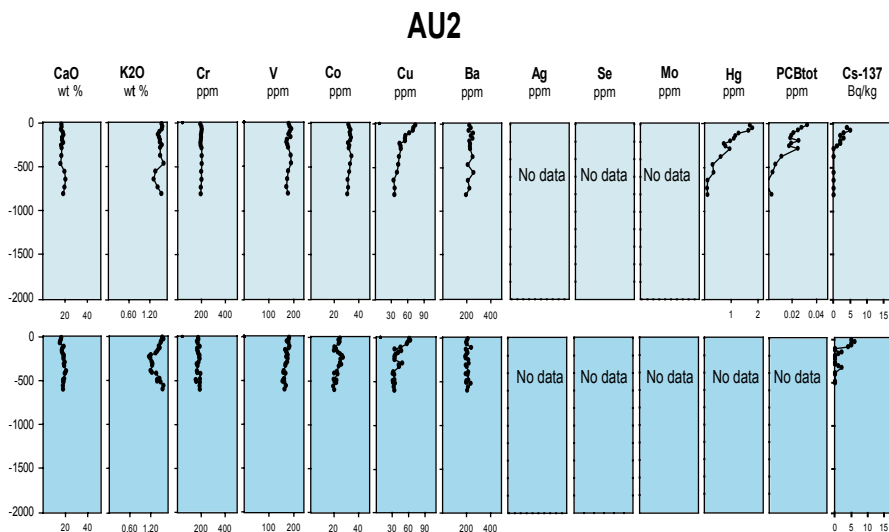


**Fig. 15.8** Elemental profiles for both AU2 cores determined by WD-XRF. Depth is shown on the y-axis in mm

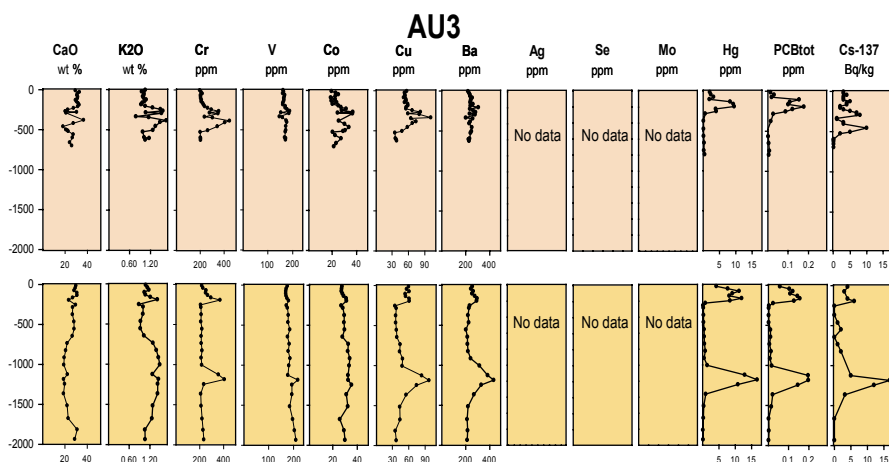


**Fig. 15.9** Elemental profiles for both AU3 cores determined by WD-XRF. Depth is shown on the y-axis in mm

**Site AU3** Grain-size shows the prevalence of fine fractions (clay and silt) throughout its length with the exception of the lower 12 cm and the upper 30 cm of the core, where sand attains values around 40% (Fig. 15.5), while the highest clay content was recorded from -60 to -150 cm. The two cores studied for sediment geochemistry (AU3<sub>g<sub>iwc</sub></sub> and AU3<sub>v<sub>cr</sub></sub>) show quite different elemental and radionuclide profiles indicating significant variations in sediment accumulation rate (10–25 mm/year). At

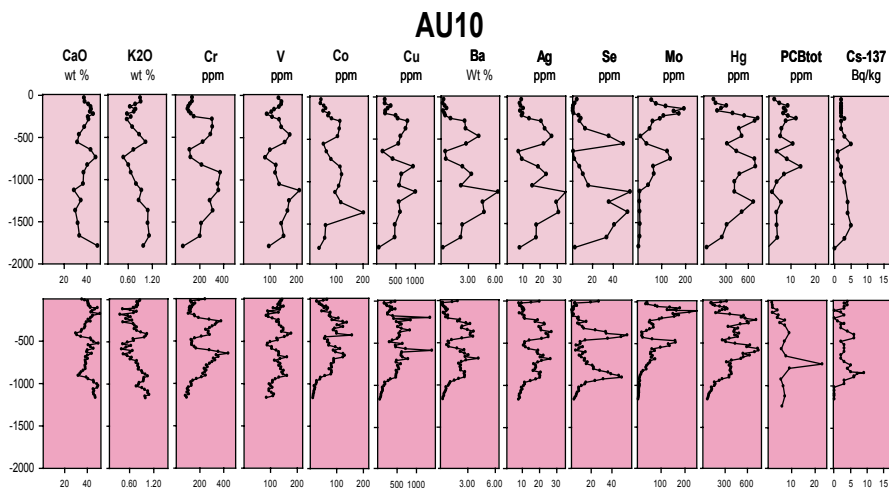


**Fig. 15.10** Elemental profiles for both AU10 cores (upper AU10v and lower AU10g) determined by WD-XRF. Depth is shown on the y-axis in mm

around  $-125$  cm the profiles of Ba, Cr, Cu, V, Hg, PCB and  $^{137}\text{Cs}$  show a series of distinctive positive spikes (Fig. 15.9).

**Site AU10** As regards grain-size, with the exclusion of levels deeper than 180 cm where gravel is prevailing, silt-size material is the most abundant fraction throughout the investigated sediment depth, with values around 50%. All the collected cores from this location (AU10<sub>g<sub>iwc</sub></sub>, AU10<sub>v<sub>iwc</sub></sub> and AU10<sub>v<sub>er</sub></sub>) show the highest concentrations of anthropogenic components (notably Ba, Hg and PCBs). Core AU10<sub>v<sub>iwc</sub></sub> was examined both non-destructively (Figs. 15.3 and 15.7) and destructively (Figs. 15.6, 15.7, 15.10 and 15.11). The analysed cores show the highest amounts of anthropogenic contamination with PCBs ( $20 \text{ mg kg}^{-1}$ ), Ba (up to 5 wt%) and Hg (up to  $600 \text{ mg kg}^{-1}$ ).

## Discussion

### *Sediment Accumulation Rates Based on $^{137}\text{Cs}$ Distributions*

Caesium-137 dating was applied to all the seven cores of this study. Lead-210 dating was also carried out on three of the cores but the complex interplay between sediment composition and activity made its straightforward application somewhat difficult. The  $^{137}\text{Cs}$  dating method uses a set of indicator features viz: the first appearance of  $^{137}\text{Cs}$  ( $\sim 1954$ ) and the 1963 ‘bomb’ maximum (Ritchie and McHenry 1990; Appleby and Oldfield 1994). The possible downward migration or mixing of

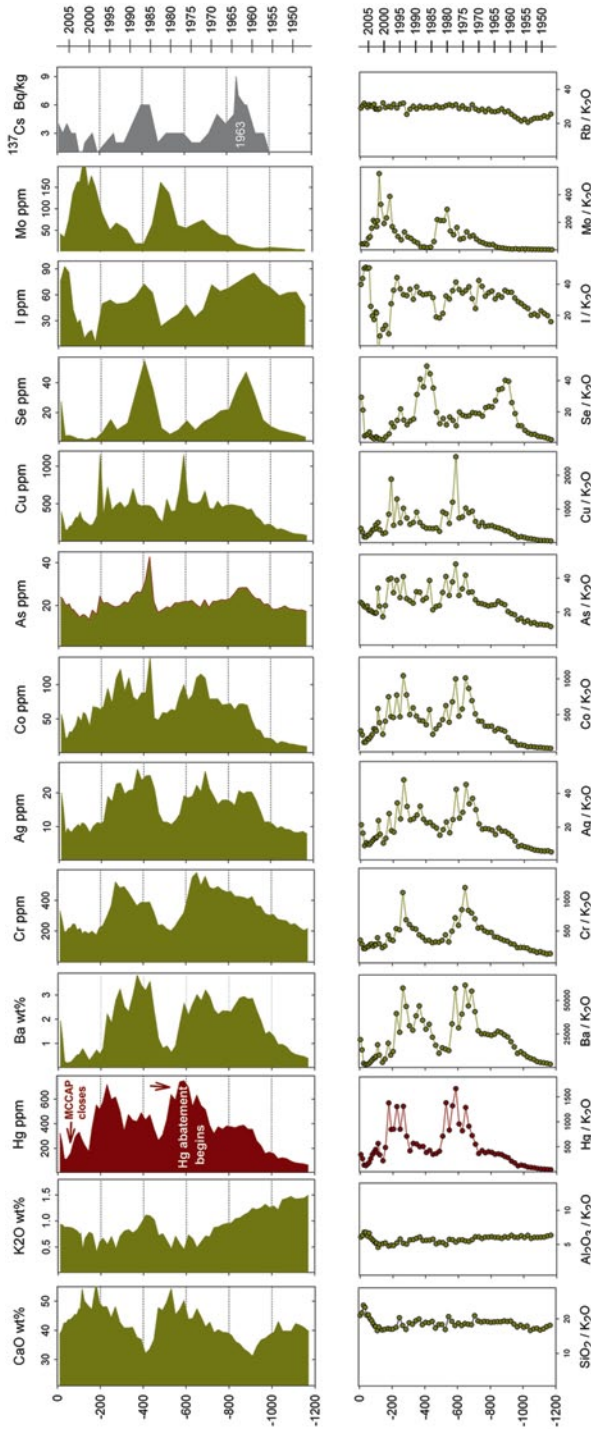


**Fig. 15.11** Elemental profiles for AU10vib at 1cm resolution determined by WD-XRF. The chronology is based on Cs-137 dating and is consistent with known historical events such as the MCCAP start-up, the introduction of mercury abatement (~ 1977–1979) and the Plant closure in 2005. Depth is shown in mm on the y-axis. Down-core elemental changes, normalised to K<sub>2</sub>O, are shown to enable clearer visualisation arising to the closed-sum effect caused by significant variations in carbonate (CaO)

**Table 15.3** Sediment accumulation rates estimated from  $^{137}\text{Cs}$  profiles (this study)

Core	Coring date	1954 (mm/year)	1963 (mm/year)	1986 (mm/year)
AU2g <sub>iwc</sub>	July 2008	7.1	7.2	6.6
AU2g <sub>er</sub>	July 2008	4.2	4.9	7.0
AU3g <sub>iwc</sub>	July 2008	9.7	10.1	13.4
AU3v <sub>er</sub>	July 2008	25.9	26.3	25.5
AU10g <sub>iwc</sub>	July 2008	Core too short	~24.4	25.6 <sup>a</sup>
AU10v <sub>iwc</sub>	July 2008	33.1	33.7	25.2
AU10v <sub>er</sub>	July 2008	18.1	19.2	19.8

The 1954, 1963 and 1986 dates represent key events in global and European  $^{137}\text{Cs}$  deposition

<sup>a</sup> This accumulation rate represents a reconsidered value from that quoted in the earlier report to ISPRA

$^{137}\text{Cs}$  has a potential impact when using the first appearance criterion only. In some parts of Europe, an additional peak corresponding to the Chernobyl event (1986) is also seen (e.g. Miller et al. 2014, 2015) but the impact of Chernobyl is generally claimed to be low in Sicily, but is not necessarily absent (Cundy et al. 1998).

The Augusta sediment core profiles show that the different cores present widely varying sediment accumulation rates ranging from 4 to 33 mm/year based on first appearance of  $^{137}\text{Cs}$  and the location of the 1963 maximum. A peak at a higher level in the cores is potentially related to Chernobyl input but the observation that  $^{137}\text{Cs}$  also varies positively with sediment composition (K and Rb) means that the peak may simply corresponds to a co-incidental increase in a clay mineralogical control (see Figs. 15.4, 15.5, 15.8, 15.9, 15.10 and 15.11). This effect complicates the normal application of the method and care is needed in not simply equating maxima with features such as the 1963 bomb peak. Perhaps the most notable difference is the significantly higher accumulation rates found in cores collected around site AU10.

AU2: Both cores show low accumulation rates of 4–7 mm/year.

AU3: The two cores collected show quite different accumulation rates (~10 and ~26 mm/year) although the  $^{137}\text{Cs}$  profiles do show some similar features.

AU10: These three cores from this site show accumulation rates varying from 20, 25 to 33 mm/year. The only core run on the Itrax (AU10v<sub>iwc</sub>), although similar to the other cores from the AU10 location, shows clear and persistent compositional layering (see the radiograph of Fig. 15.3). The layers correlate with variations in K and Ca (Fig. 15.3) which indicate variations in clay and carbonate components (Table 15.3).

### ***Geochemical Variations: Itrax Vs WD-XRF***

There is a clear similarity in the geochemical profiles recorded using high-resolution Itrax scanning (data in counts) and those obtained using the quantitative WD-XRF (Ca, K, Fe, Ba, Sr, Hg, Zn, Cu, Cr, Se, Br, Cr, Fig. 15.7). This confirms the capability of X-ray core scanner to record reliable geochemical variations.

- The Itrax system scanning resolution is able to identify high frequency geochemical changes that can be missed with lower resolution (1-cm scale) conventional analysis.
- The speed and sensitivity of the Itrax analytical method provides broad range elemental variation data (Si–U) from normal levels through to anthropogenic enrichments.
- The simultaneously acquired high-resolution radiographic image(s) provides a powerful visual insight into sediment layering that corresponds to mineralogical and density changes. In some cores these may be inferred to have climatological significance (e.g. Miller et al. 2014, 2015).

### ***Geochemical Variations with Location***

The geochemical data of the cores from the three areas show an increase in pollution going from north to south of the Harbour (AU2 to AU3 to AU10; Figs. 15.8, 15.9, 15.10 and 15.11). The main anthropogenic components (see Table 15.2) are Ag, Ba, Ca, Hg, Co, Cr, Cu, Mo, Zn, PAHs and PCBs. Heavy metal concentrations in cores collected from AU2 and AU3 are of the same order of magnitude while the concentrations in cores from the AU10 location are considerably elevated and reflect their close proximity to the main sources of contamination. A general feature of all cores is a covariation in the amount of anthropogenic contaminants. The major spikes could be explained in some cases through redox processes but the time required for such adjustments could be considerable in subtidal sediment (Thomson et al. 1993). The variations seen in Augusta Harbour are dominated by solid phase pollution inputs that became incorporated into the accumulating sediment but a case for some redox adjustment could be made for some elements (e.g. Mn, Se and Mo).

**Site AU2** The two cores collected from this site have a largely similar geochemistry and accumulation rates in the range 5–7 mm/year. Evidence of anthropogenic inputs (notably Hg and PCBs) first appear around –50 cm and generally increase to the surface (Fig. 15.8).

**Site AU3** These two cores are unusual in that for each core the pollution histories are contained in 50 cm and 150 cm respectively. A question arises as to why there is this difference? The core with the thicker sequence AU3<sub>ver</sub> is unusual in showing very low concentrations at depth until a maximum at about –125 cm that then falls off again to low values (Fig. 15.9). A similar pattern is seen for other anthropogenic elements and unusually also <sup>137</sup>Cs. The covariation and the sharp rise and fall of Cr, Cu, Ba, Hg, PCB and <sup>137</sup>Cs could be explained if the sediment sequence included a significant thickness due to the dumping of old, mixed contaminated waste at this site.

**Site AU10** The concentration profiles of cores from AU10 site show different characters with respect to the other cores. Although the lowest concentrations are recorded at the core bottom, values both for trace elements and organic compounds at this level are already very high (Figs. 15.10 and 15.11). This indicates that bottom sediments were deposited after the onset of the petrochemical centre. Downcore

a clear trend is not distinguishable, although two main peaks around –80 cm and slightly below 20 cm depth are common to PCBs. All contaminants, with exception of Ba, show a decrease in the upper 20 cm, although concentrations at the top are still extremely high for all contaminants. The significant variations in CaO for Augusta cores lead to profiles that reveal the closed-sum effect. In other words since major element data sum to 100% where a component varies significantly there are corresponding variations seen in other components (Rollinson 2009). The use of ratios can suppress the closed-sum effect and typical divisors used are Al, K, Rb and Ti. In this study, based on observed elemental co-variations,  $K_2O$  was used.

### *Anthropogenic Inputs*

**Barium and Calcium** Barium concentrations in all cores from AU10 are significantly higher than are found in typical marine sediments (Table 15.2). The close correlation with S, the high concentration and the observation of finely dispersed white grains in dried sediment shows that the high Ba is due to anthropogenic barite ( $BaSO_4$ ). This is inferred to be a precipitate produced during brine purification linked to the MCCAP process. Chemical impurities in the brines (e.g. Ca, Mg and sulphate) were well known to have an adverse effect on the electrolytic process and were removed to avoid formation of so-called ‘mercury butter’. This undesirable product would have led to short circuits, poor mercury flow, increased power consumption and increased exposure to mercury vapour (Text Box 15.2). The removal of sulphate was usually achieved by adding soluble  $BaCl_2$  to create a barite precipitate.

The identification of significant barite in the AU10 core profiles shows that the brine purification wastes must have been discharged into the harbour. It might be anticipated that there would be a general correlation between Ba and Hg since their coexistence was linked to the MCCAP. However, the profile data show a slight mismatch suggesting a separate waste stream.

Calcium concentrations are significantly higher in the southernmost cores at site AU10 than in the other cores further north. Although carbonate is a significant natural component of the sediment it appears that the elevated Ca seen in Core AU10 (polluted) compared with ore AU2 (relatively unpolluted) could reflect an anthropogenic component. This might be due to  $CaSO_4$  precipitates from the brine purification process.

**Mercury** Mercury is broadly recognized as a pernicious environmental pollutant and international agreements (co-ordinated through UNEP) have pledged to progressively eliminate it from virtually all industrial use (Text Box 15.2). In the past MCCAPs have been a significant source of mercury to the environment (Anirudh et al. 2009). The highest Hg concentration recorded in each core location are AU2 ( $1.8 \text{ mg kg}^{-1}$ ), AU3 ( $17 \text{ mg kg}^{-1}$ ) and AU10 ( $728 \text{ mg kg}^{-1}$ ).

The Hg profiles for the most contaminated cores (AU10; Figs. 15.3, 15.10 and 15.11) show a progressive rise from the early 1950s up to a maximum around 1977. This maximum corresponds closely to the introduction of mercury abatement around 1979. The decline in Hg persists until around 1984 whereupon there is an

increase to another maximum corresponding to around 1994. There is currently no evidence to explain this increase but a speculation could be that unauthorized discharges occurred. By 2005 the MCCAP had finally closed and the mercury cells removed. Overall, the variations in Hg concentrations, when linked to the  $^{137}\text{Cs}$  chronology, accord with the main historical records (*viz.* inception of MCCAP, introduction of Hg abatement measures and final plant closure).

**Selenium** The geochemical profile for Augusta core AU10 shows two distinct peaks in Se reaching nearly  $50 \text{ mg kg}^{-1}$ . This selenium is likely to have an industrial origin since normal marine (carbonate or clay rich) sediments typically only contain up to  $1 \text{ mg kg}^{-1}$ . There are two plausible sources. One could be linked to materials derived from a mercury vapour capture technology that could have been used in the chlor-alkali plant (MCCAP). Selenium scrubbing is a wet media process for removal of fairly large quantities of mercury from flue gases. The gaseous mercury reacts with activated amorphous selenium, which is circulating in a scrubber with a 20–40% sulphuric acid. The mercury removal efficiency is claimed to be greater than 90% and the product is insoluble mercury selenide (Hagemann 2009). Another, more probable origin of the Se is from crude oil processed in the petrochemical industry as it is reported to contain relatively high concentrations (up to  $2200 \mu\text{g/L}$  of Se; Lemly 2002).

**Chromium, Cobalt and Molybdenum** Co, Cr and Mo are elevated in Augusta sediment and are particularly evident in AU10. Chromium exists up to five times above muddy sediment concentrations (Table 15.2). The most likely explanation for this combination of elements in the harbour sediment is that they originate from discharges of waste catalyst used in petrochemical processes (desulphurization and cracking). Hydrodesulphurisation is commonly used in petrochemical refineries to remove sulphur for environmental and health reasons. The process involves passing crude oil and hydrogen over a catalyst at elevated T and P to convert any organic sulphur (commonly up to ~2.5%) to hydrogen sulphide. So-called CoMOX catalysts (typically 3–5% cobalt oxide and 14%  $\text{MoO}_3$  immobilised on  $\text{Al}_2\text{O}_3$ ) are used as they are resistant to poisoning and degradation and can be regenerated and re-used for several years. Large quantities of spent hydrodesulfurization (HDS) catalysts are produced by the industry. Disposal of spent catalyst is a problem as it falls under the category of hazardous industrial waste. In recent times the value of these spent materials is recognized and recycling can be carried out (Rojas-Rodríguez et al. 2012) but in earlier, less environmentally sensitive times, it may have been considered more convenient to simply dispose of the spent catalyst into the Harbour.

**Copper** Cores from AU10 show sharp inflections in Cu, particularly in the core scanned by the Itrax and then sampled at high resolution. The sharp peaks approximately coincide with broader Hg and Cr peaks. It is unclear whether Cu had any role in the MCCAP. It is more likely that it was linked to refinery processes since it is known that copper chloride mixed with clay was widely used as a sweetening agent to remove malodorous mercaptans (organo-sulphur compounds) during oil refinery processing (Croudace and Cundy 1995).

**PCBs** Organic pollutants in the Harbour are derived from the longstanding petrochemical operations from the early 1950s to the current time. The main PCB

present is PC209 that is highly correlated with Hg concentration possibly indicating a link to the Chlor-alkali plant. Sediment from AU2 and AU3 has similar median values of  $0.019 \text{ mg kg}^{-1}$  and  $0.0016 \text{ mg kg}^{-1}$  respectively. Sediment from AU10 has concentrations several orders of magnitude higher with median values of 6.2 and  $2.1 \text{ mg kg}^{-1}$  respectively. The concentration profiles of core AU10 show different characters with respect to the other cores. Although the lowest concentrations are recorded at the core bottom, values at this level are already very high (Fig. 15.11). This indicates that bottom sediments were deposited after the onset of the petrochemical centre. Along depth a clear trend is not distinguishable, although two main peaks around  $-80 \text{ cm}$  and slightly below  $-20 \text{ cm}$  depth are common to PCBs.

**Silver** Core AU10 shows measurable silver (WDXRF measurements). The co-variation with Ba may indicate a probable link to wastes discharges from the MCCAP.

### *Understanding the Geochemical Profiles*

Down-core elemental profiles for cores AU2 (AU2<sub>g<sub>iwc</sub></sub> and AU2<sub>v<sub>er</sub></sub>) and AU3<sub>g<sub>iwc</sub></sub> are generally similar and do not reveal high pollution showing that they are some distance from the main effluent input. The main characteristic features for the  $^{137}\text{Cs}$  records are largely synchronous with the early industrial evolution of the area and they are all evident above  $-50 \text{ cm}$ . Core AU3<sub>v<sub>er</sub></sub> is more unusual in showing a set of peaks at approximately  $-125 \text{ cm}$  for elements that are expected to be independent of each other (Cr, V, Cu, Ba, Hg, PCB, and  $^{137}\text{Cs}$ ). The sharp rise followed by the rapid fall could be explained by relatively unpolluted dredge spoils being dumped near AU3 around 1965. The fact that geochemically unrelated components all have a peak at the same location might indicate the dumping of mixed material of early 1960s.

The cores from AU10 show similar geochemical variations to each other but are distributed over different sediment thicknesses. AU10<sub>v<sub>iwc</sub></sub> has accumulated approximately  $120 \text{ cm}$  whereas AU10<sub>v<sub>er</sub></sub> has accumulated  $220 \text{ cm}$  sediment. This variation could be explained by variations in bottom topography (Anonymous 1992, 1995). The geochemical profiles for AU10<sub>v<sub>iwc</sub></sub> data show patterns clearly affected by variations in the calcium carbonate mineral component. After normalisation ( $\text{K}_2\text{O}$ ) elemental pollutant profiles are simplified but essentially show similar features to the non-normalised profiles (Fig. 15.7).

### **Conclusions**

The considerable pollution legacy in Augusta Harbour has been a focus of interest for regulators and authorities interested in wholesale remediation to European standards. The current geochemical investigation has provided an excellent opportunity to evaluate the usefulness of the Itrax core scanner as an environmental forensic analytical tool. The Itrax data were validated against a conventional WD-XRF dataset and found to accurately reflect the elemental variations for a broad range of major, minor and trace elements.

Additional to the Itrax data, a range of other geochemical data were acquired including PCBs, PAHs, Hg, Ba, Cr, Cu and  $^{137}\text{Cs}$  and their variations were used to evaluate the timing of pollutant inputs. The Itrax radiographic image, when correlated with particle size data and XRF major elements (Ca and K) helped provide an insight into the composition of sediment layers.

Unusual enrichments of elements seen in the most polluted site (AU10) are interpreted as waste materials discharged into the Harbour during industrial operations.

- Ba (and Ca in part)—originate from the brine purification process linked to the MCCAP
- Hg—a waste element derived from inefficiencies in the MCCAP electrolytic process
- Cr, Co, Mo, (V)—derived from disposal of waste catalysts used in oil refineries
- Cu—linked to oil refinery operations (e.g. sweetening of gases)
- Se—ultimately derived from crude oil (Lemly 2002)
- Ag—likely to be related to the operations at the MCCAP based on co-variation with Ba

One of the key interests of the Italian Environmental Prosecutor was to reconcile variations in anthropogenic elements, particularly mercury, with specific polluting companies. This required a reliable sediment chronology and  $^{137}\text{Cs}$  dating was employed and found to provide a timescale consistent with known pollution events. In the most contaminated cores from site AU10 steep early changes in Hg, Ba and other anthropogenic components are linked to the known rapid expansion in the MCCAP and petroleum refining in the early 1950s. Around 1977 there is a decline in Hg that links to the known introduction of a mercury abatement process. From 1992 to 1997 Hg concentrations increase again to another maximum before they finally decline which links to the ultimate closure of the MCCAP in 2005. The increase seen from 1992 to 1997 could be associated with unauthorized discharges.

The ITRAX investigation of Augusta sediments has made a valuable contribution to this environmental forensic study. The geochemical variations seen in the most polluted core have been validated by comparing data obtained using conventional (quantitative) WD-XRF. The speed and resolution of ITRAX analysis are clear strengths of this method. As in all geochemical studies where significant variations in major components occur, consideration of the closed-sum effect should be taken into account to avoid misinterpretation of elemental profiles.

## References

- Anirudh R, Rokade MA, Zingde MD, Borole DV (2009) Post-depositional memory record of mercury in sediment near the effluent disposal site of a chloralkali plant in Thane Creek–Mumbai Harbour, India. *Environ Technol* 30:765–783
- Anonymous (1992) Sistema integrato per il monitoraggio automatico della rada di Augusta. I-Studi preliminari per il posizionamento di boe oceanografiche. Istituto Sperimentale Talassografico CNR Messina. *Rapporti* 6:1–120

- Anonymous (1995) Studio sedimentologico e bionomico dei fondi mobili della Rada di Augusta. Istituto Sperimentale Talassografico CNR Messina. Rapporti 9:1–72
- Appleby P, Oldfield F (1992) Application of lead-210 to sedimentation studies. In: Ivanovich M, Harmon RS (eds) Uranium-series disequilibrium: applications to earth, marine, and environmental science. Oxford University Press, pp 731–738
- Ausili A, Gabellini M, Cammarata G, Fattorini D, Benedetti M, Pisanelli B, Gorbi S, Regoli F (2008) Ecotoxicological and human health risk in a petrochemical district of southern Italy. *Mar Environ Res* 66:215–217
- Ausili A, Cappucci S, Gabellini M, Innocenti C, Maffucci M, Romano E, Rossi L, Taramelli A (2012) New approaches for multi source data sediment characterisation, thickness assessment and clean-up strategies. *Chem Eng Trans* 28:223–228
- Bellucci LG, Giuliani S, Romano S, Albertazzi S, Mugnai C, Frignani M (2012) An integrated approach to the assessment of pollutant delivery chronologies to impacted areas: Hg in the Augusta Bay (Italy). *Environ Sci Technol* 46:2040–2046
- Bergamin L, Romano E, Finoia MG, Venti F, Bianchi J, Colasanti A, Ausili A (2009) Benthic foraminifera from the coastal zone of Baia (Naples, Italy): assemblage distribution and modification as tools for environmental characterisation. *Mar Pollut Bull* 59:234–244
- Bianchi F, Bianca S, Linzalone N, Madeddu A (2004) Sorveglianza delle malattie congenite in Italia: un approfondimento nella provincia di Siracusa. *Epidemiol Prev* 28:87–93
- Bonsignore M, Salvagio D, Manta E, Oliveri M, Sprovieri M, Basilone G, Bonanno A, Falco F, Traina A, Mazzola S (2013) Mercury in fishes from Augusta Bay (southern Italy): risk assessment and health implication. *Food Chem Toxicol* 56:184–194
- Castagna A, Sinatra F, Castagna G, Stoli A, Zafarana S (1985) Trace element evaluations in marine organisms. *Mar Pollut Bull* 16:416–419
- Cearreta A, Ulibarra I, Irabien MJ, Yusta L, Leorri E, Croudace IW, Cundy AB (2002) Recent salt marsh development and natural regeneration of reclaimed areas in the Plentzia estuary, N. Spain. *Estuar Coast Shelf Sci* 54:863–886
- Celia Magno M, Bergamin L, Finoia MG, Pierfranceschi G, Venti F, Romano E (2012) Correlation between textural characteristics of marine sediments and benthic foraminifera in highly anthropogenically-altered coastal areas. *Mar Geol* 315–318:143–161
- Cernigliaro A, Addario SP, Nicolotti N (2008) Research on the health state of the Sicilian population living in areas at environmental or natural risk: the experience of the Regional Department of Epidemiology. *Ital J Public Health* 5:80–85
- Clarkson T (1997) The toxicology of mercury. *Crit Rev Clin Lab Sci* 34:369–403
- Covelli S, Faganelli J, Horvat M, Brambati A (2001) Mercury contamination of coastal sediments as the result of long-term cinnabar mining activity (Gulf of Trieste, northern Adriatic sea). *Appl Geochem* 16:541–558
- Covelli S, Acquavita A, Piani R, Predonzani S, De Vittor C (2009) Recent contamination of mercury in an estuarine environment (Marano lagoon, Northern Adriatic, Italy). *Estuar Coast Shelf Sci* 82:273–284
- Covelli S, Emili A, Acquavita A, Dinelli E, Koron N, Faganelli J (2010) Benthic fluxes measurement of mercury and methylmercury in Pialassa Baiona (Ravenna, Italy). *Int J Environ Qual (EQA)* 3:33–40
- Croudace IW, Cundy AB (1995) A record of heavy metal pollution in recent sediments from Southampton Water, Southern England: a geochemical and isotopic study. *Environ Sci Technol* 29:1288–1296
- Croudace IW, Rothwell RG (2015) Future developments and innovations in high-resolution core scanning in IW Croudace. In: Rothwell RG (ed) *Micro-XRF studies of sediment cores*. Springer, Netherlands
- Croudace IW, Rindby A, Rothwell RG (2006) Itrax: description and evaluation of a new sediment core scanner. In: Rothwell RG (ed) *New techniques in sediment core analysis*. Geol Soc Spec Publ, London, 267:51–63

- Croudace IW, Warwick PE, Morris JE (2012) Evidence for the preservation of technogenic triated organic compounds in an estuarine sedimentary environment. *Environ Sci Technol* 46:5704–5712
- Cundy AB, Collins PEF, Turner SD, Croudace IWC, Horne D (1998) 100 years of environmental change in a coastal wetland. Augusta Bay, southeast Sicily: evidence from geochemical and palaeoecological studies. *Geol Soc Lond Spec Publ* 139:243–254
- Cundy AB, Croudace IW, Cearreta A, Irabien MJ (2003) Reconstructing historical trends in metal input in heavily-disturbed, contaminated estuaries: studies from Bilbao, Southampton Water and Sicily. *Appl Geochem* 18:311–32
- Di Leonardo R, Bellanca A, Capotondi L, Cundy A, Neri R (2006) Possible impacts of Hg and PAH contamination on benthic foraminiferal assemblages: an example from the Sicilian coast, central Mediterranean. *Sci Total Environ* 388:168–183
- Di Leonardo R, Adelfio G, Bellanca A, Chiodi M, Mazzola S (2014) Analysis and assessment of trace element contamination in offshore sediments of the Augusta Bay (SE Sicily): a multivariate statistical approach based on canonical correlation analysis and mixture density estimation approach. *J Sea Res* 85:428–442
- Govindaraju K (1994) Compilation of working values and sample description for 383 geostandards. *Geostand News* 18:1–158
- Guerriero C, Bianchi F, Cairns J, Cori L (2011) Policies to clean-up toxic industrial contaminated sites of Gela and Priolo: a cost-benefit analysis. *Environ Health* 10:68 (Open Access)
- Hagemann S (2009) GRS—252 Oktober 2009 Gesellschaft für Anlagen und Reaktor sicherheit (GRS), GmbH. GRS—252 ISBN 978-3-939355-27-4. [http://ec.europa.eu/environment/air/pdf/pp\\_mercury7.pdf](http://ec.europa.eu/environment/air/pdf/pp_mercury7.pdf). Accessed Sept 2013
- Hester RE, Harrison RM (eds) (2008) Environmental forensics. *Issues in Environmental Science and Technology*. RSC Publ, London, pp 190
- ICRAM (2008) Progetto preliminare di bonifica della rada di Augusta inclusa nel sito di bonifica di interesse nazionale di Priolo Fase I e Fase II. Report. BoI-Pr-SI-PR-Rada di Augusta-03.22, Internal Report
- Lemly AD (2002) Selenium assessment in aquatic ecosystems: a guide for hazard evaluation and water quality criteria. Springer, New York
- Lepland A, Andersen TJ, Lepland A, Arp HP, Alve E, Breedveld GD, Rindby A (2010) Sedimentation and chronology of heavy metal pollution in Oslo harbour, Norway. *Mar Pollut Bull* 60:1512–1522
- Maggi C, Berducci MT, Bianchi J, Giani M, Campanella L (2009) Methylmercury determination in marine sediment and organisms by direct mercury analyser. *Anal Chim Acta* 641:32–36
- Miller H, Croudace IW, Bull JM, Cotterill JC, Dix JK, Taylor RN (2014) A 500 year sediment lake record of anthropogenic and natural inputs to Windermere (English Lake District) using double-spike lead isotopes, radiochronology, and sediment microanalysis. *Environ Sci Technol* 48:7254–7263
- Miller H, Croudace IW, Bull JM, Cotterill CJ, Taylor RN (2015) Modern pollution signals in sediments from Windermere, NW England, determined by micro-XRF and lead isotope analysis. In: Croudace IW, Rothwell RG (eds) *Micro-XRF studies of sediment cores*. Springer, Netherlands
- Nigro F, Renda P (2000) Un modello di evoluzione tettono-sedimentaria dell'avanfossa neogenica Siciliana. *Boll Soc Geol Ital* 119:667–686
- Piani R, Covelli S, Biester H (2005) Mercury contamination in Marano Lagoon (Northern Adriatic Sea, Italy): source identification by analyses of Hg phases. *Appl Geochem* 20:546–1559
- Raldúa D, Díez S, Bayona JM, Barceló D (2007) Mercury levels and liver pathology in feral fish living in the vicinity of a mercury cell chlor-alkali factory. *Chemosphere* 66:1217–1225
- Ritchie JC, McHenry JR (1990) Application of radioactive fallout cesium-137 for measuring soil erosion and sediment accumulation rates and patterns: a review. *J Environ Qual* 19:215–233
- Rojas-Rodríguez AD, Flores-Fajardo O, González FSA, Castillo NNL, Gómez MJC (2012) Chemical treatment to recover molybdenum and vanadium from spent heavy gasoil hydrodesulfurization catalyst. *Adv Chem Eng Sci* 2:408–412

- Rollinson HR (1993) Using geochemical data: evaluation, presentation, interpretation. Pearson Harlow, Longman
- Romano E, Bergamin L, Ausili A, Pierfranceschi G, Maggi C, Sesta G, Gabellini M (2009a) The impact of the Bagnoli industrial site (Naples, Italy) on sea-bottom environment. Chemical and textural features of sediments and the related response of benthic foraminifera. *Mar Pollut Bull* 59:244–255
- Romano E, Bergamin L, Finoia MG, Celia Magno M, Ausili A, Gabellini M (2009b) The effects of human impact on benthic foraminifera in the Augusta harbour (Sicily, Italy). In: Dahl E, Moksness E, Støttrup, J (eds), Proceedings of the International Symposium on Integrated Coastal Zone Management. Wiley-Blackwell, Chichester, pp 97–115
- Romano E, Bergamin L, Celia Magno M, Ausili A (2013) Sediment characterization of the highly impacted Augusta harbour (Sicily, Italy): modern benthic foraminifera in relation to grain-size and sediment geochemistry. *Environ Sci Process Impacts* 15:930–946
- Sciacca S, Fallico R (1978) Presenza e concentrazione di sostanze inquinanti di origine industriale nella Rada di Augusta (Siracusa). *Inquinamento* 20(6):33–38
- Scicchitano G, Monaco C, Tortorici L (2007) Large boulder deposits by tsunami waves along the Ionian coast of south-eastern Sicily (Italy). *Mar Geol* 238:75–91
- Sedivy VM (2009) Environmental balance of salt production speaks in favour of solar saltworks. *Glob NEST J* 11:41–48
- Sproveri M, Oliveri E, Di Leonardo R, Romano E, Ausili A, Gabellini M, Barra M, Tranchida G, Bellanca A, Neri R, Budillon F, Saggiomo R, Mazzola S, Saggiomo V (2011) The key role played by the Augusta basin (southern Italy) in the mercury contamination of the Mediterranean Sea. *J Environ Monit* 13:1753–1760
- Thomson J, Higgs NC, Croudace IW, Colley S, Hydes DJ (1993) Zonation of redox-sensitive elements at the oxic/post-oxic interface in deep-sea sediments. *Geochim Cosmochim Acta* 57:579–595
- Tomiyasu T, Matsuyama A, Eguchi T, Fuchigami Y, Oki K, Horvat M (2006) Spatial variations of mercury in sediment of Minamata Bay, Japan. *Sci Total Environ* 368:283–290
- WHO (2012) Biomonitoring-based indicators of exposure to chemical pollutants. Report of a meeting Catania, Italy, 19–20 April 2012, WHO Report (Europe), Regional Office for Europe, Copenhagen, Denmark